Published in final edited form as:
Cell Rep. 2014 January 16; 6(1): 196–210. doi:10.1016/j.celrep.2013.12.014.

Dual engagement of the NLRP3 and AIM2 inflammasomes by plasmodial-derived hemozoin and DNA during malaria

Parisa Kalantari[1], **Rosane B. DeOliveira**[1,&], **Jennie Chan**[1,&], **Yolanda Corbett**[2], **Vijay Rathinam**[1], **Andrea Stutz**[3], **Eicke Latz**[1,3], **Ricardo T. Gazzinelli**[1,4], **Douglas T. Golenbock**[1,*], and **Katherine A. Fitzgerald**[1,*]

[1]Division of Infectious Diseases and Immunology, University of Massachusetts Medical School, Worcester, MA, USA 01605

[2]Dipartimento di Scienze Farmacologiche e Biomolecolari Universita Degli Studi di Milano, Via Pascal 36, Milano 20133, Italy

[3]Institute of Innate Immunity, Biomedical Center, 1G008, University Hospitals, University of Bonn, Sigmund-Freud-Str. 25, Bonn 53127, Germany

[4]Department of Parasitology and Department of Biochemistry and Immunology, Biological Sciences Institute, Federal University of Minas Gerais, Av. Antonio Carlos 6627, Belo Horizonte, MG 31270, Brazil

SUMMARY

Hemozoin (Hz) is the crystalline detoxification product of hemoglobin in plasmodial-infected erythrocytes. We previously proposed that Hz can carry plasmodial DNA into a subcellular compartment accessible to Toll-like receptor 9 (TLR9), inducing an inflammatory signal. Hemozoin also activates the NLRP3 inflammasome in primed cells. We found that Hz appears to co localize with DNA in infected erythrocytes, even prior to RBC rupture or phagolysosomal digestion. Using synthetic Hz coated *in vitro* with plasmodial genomic DNA (gDNA) or CpG-oligonucleotides, we observed that DNA-complexed Hz induced TLR9 translocation, providing a priming and an activation signal for inflammasomes. After phagocytosis, Hz and DNA dissociate. Hz subsequently induces phagolysosomal destabilization, allowing phagolysosomal contents

Correspondence should be addressed to: Katherine A. Fitzgerald, Division of Infectious Diseases and Immunology, University of Massachusetts Medical School, Worcester, MA 01605. (ph) 508.856.6518, (fax) 508.856.8447, kate.fitzgerald@umassmed.edu or D.T.G., douglas.golenbock@umassmed.edu.
*&These authors contributed equally to this work.

Supplemental information
Supplemental information includes 6 figures.

Author Contributions
K.A.F, D.T.G and R.T.G oversaw the whole project. P.K. designed and conducted the experiments with help from R.D., J.C., A.S. and V.R. Preparation of nHz was done by Y.C. P.K., K.A.F. and D.T.G wrote the manuscript.

Competing financial interest
The authors declare no competing financial interest.

access to the cytosol where DNA receptors become activated. Similar observations were made with plasmodial-infected RBC. Finally, infected erythrocytes activated both the NLRP3 and AIM2 inflammasomes. These observations suggest that Hz and DNA work together to induce systemic inflammation during malaria.

INTRODUCTION

Malaria continues to be one of the most devastating global health problems in human history. The overwhelming majority of cases of life-threatening malaria are caused by infection with *Plasmodium falciparum* (*Pf*), mostly in children under 5 (Snow et al., 2005). *Plasmodium spp*. replicate inside red blood cells. The rupture of parasitized red blood cells induces a pro-inflammatory cytokine storm that coincides with fever in malaria patients (Grau et al., 1989; Kwiatkowski and Nowak, 1991). Excessive production of several cytokines, including tumor necrosis factor (TNF)α (Grau et al., 1989; Kwiatkowski et al., 1990), interferon gamma (IFNγ) (Grau et al., 1989), interleukin (IL)-12 (Grau et al., 1989) and IL-1β (Franklin et al., 2009) have all been linked to disease. IL-1β is a highly synergistic cytokine, and its regulation has the potential to radically modify the expression and the effects of other immunomodulators (Last-Barney et al., 1988; Stashenko et al., 1987).

Several components of the *Plasmodium* parasite have been proposed to act as ligands for host receptors (Gazzinelli and Denkers, 2006). Parasite DNA represents a major trigger of innate immunity during infection. The genome of *Plasmodium* contains highly stimulatory CpG motifs, which activate TLR9 (Parroche et al., 2007). *Plasmodium* CpG DNA stimulates TLR9 via Hz (Gowda et al., 2011; Parroche et al., 2007; Pichyangkul et al., 2004), which enhances delivery of DNA into the lysosomal compartment to engage this receptor. A protein-DNA complex from the parasite has also been shown to activate TLR9 independently of Hz through (Wu et al., 2010). The genome of *Plasmodium* is highly AT-rich (Gardner et al., 2002). An AT-rich stem-loop motif that is present in abundance in both *P. falciparum* and *P. vivax* has been shown to engage a cytosolic DNA sensing pathway involving STING, TBK1 and IRF3 (Sharma et al., 2011). As a result of the proteolysis of hemoglobin in the digestive vacuole of the parasite, toxic heme accumulates. Plasmodial species have the capability to polymerize heme into the inert crystal Hz inside their food vacuole. This crystal is released from infected erythrocytes during schizogeny. Once liberated, Hz is rapidly phagocytosed by immune cells where it activates SRC-kinases (Shio et al., 2009) and induces the production of pro-inflammatory cytokines (Barrera et al., 2011; Jaramillo et al., 2005; Pichyangkul et al., 1994; Sherry et al., 1995). Hemozoin is often “synthesized” in the laboratory from hemin. In contrast to synthetic Hz (sHz), natural Hz (nHz) prepared from *Pf* cultures is bound by proteins and plasmodial DNA (Parroche et al., 2007). The immunological activity of pure Hz (*i.e*., sHz that has no hemin-associated contaminants) is controversial.

Hz has been proposed to be a ligand for TLR9 (Coban et al., 2005). Our group found that the TLR9-stimulatory capacity of nHz was dependent on *Plasmodium* DNA on the surface of the crystal, and not the Hz itself (Parroche et al., 2007). Although the transcriptional activity of Hz required the presence of surface DNA, Hz does have immunological activity.

Synthetic Hz activates the Nod-like Receptor containing Pyrin domain 3 (NLRP3) inflammasome, resulting in the production of IL-1β and IL-18 (Dostert et al., 2009; Griffith et al., 2009; Reimer et al., 2010; Shio et al., 2009).

IL-1β mediated fever is one of the hallmarks of malaria (Brown et al., 1999; Clark et al., 1994; Clark and Rockett, 1994) and the inflammasome is central to its regulation. The inflammasome is a multi-protein complex responsible for the processing and secretion of IL-1β. Mature IL-1β production requires priming signals to induce transcription of pro-IL-1β and NLRP3, and a second signal to initiate inflammasome assembly and activation.

The NLRP3 inflammasome senses a wide range of signals (Mariathasan et al., 2004) including crystalline materials such as monosodium urate and cholesterol crystals (Duewell et al., 2010; Martinon et al., 2006). These particulates trigger lysosomal deterioration and release of lysosomal contents into the cytosol, which then activate NLRP3 (Duewell et al., 2010; Halle et al., 2008; Hornung et al., 2008). Absent in melanoma 2 (AIM2), a member of the (HIN)−200 family recognizes cytosolic double-stranded DNA (Burckstummer et al., 2009; Hornung et al., 2009; Rathinam et al., 2010).

Here, we report our findings on the molecular basis for IL-1β production in malaria. Our data suggest that DNA drives many aspects of the innate immune response during malaria, and that it gets into the phagocytic compartment of cells either through the ingestion of free Hz, which can traffic associated DNA, or the phagocytosis of Hz-laden infected RBC, where it activates TLR9. The full activity of plasmodial DNA depends on the parallel activities of Hz. We suggest that the parasite components Hz and DNA play a significant role in inflammation and tissue damage during disease.

RESULTS

DNA-coated Hz provides all of the signals necessary for NLRP3 inflammasome activation and production of mature cytokines

Our group has reported that TLR9 binds to Hz through its interaction with parasite DNA present on the surface of Hz (Parroche et al., 2007). However, it was not clear if the DNA found on the surface of nHz bound to the surface of the crystal before or after erythrocyte rupture. Hemozoin is synthesized inside the food vacuole of the parasite which is completely separate from its nucleus. During the process of parasite expansion, there is constant turnover of a subpopulation of parasites. We hypothesized that during this process of parasite turnover, Hz may be exposed to parasite DNA. In order to address this issue, we injected *P. berghei* ANKA infected mice (day 9 of infection) with BrdU, a thymidine analog that incorporates into newly synthesized DNA. After 3 injections, mice were bled. Blood was enriched to achieve a preparation of RBCs that were ~90% infected, stained with a FITC-conjugated antibody to BrdU and examined by by reflection confocal microscopy, a technique that takes advantage of the birefringence of the Hz crystal (and which we use throughout this report). Approximately 19% of the intraerythrocytic Hz crystals that were observed by confocal microscopy appeared to colocalize with BrdU (Fig. 1a, middle); while 81% did not (Fig. 1a, bottom). In addition, we found that BrdU does not interact non-specifically to nHZ (Fig. S1a). Rather, the data suggest that BrdU was incorporated into the

parasite genome, and the DNA later became associated with nHz during the natural process of parasite growth and turnover, probably due to blood derived innate immune defenses. We note that the interpretation of these studies is limited by the nature of reflection confocal microscopy, where imaging in the Z dimension is not possible.

We have previously suggested that Hz enables CpG motifs in plasmodial DNA to activate TLR9 within the phagolysosome (Parroche et al., 2007). These initial studies suggested that nHz triggered TLR9 translocation. In order to test this idea, we made sHz/DNA complexes and then assessed the fate of the DNA and sHz by reflection confocal microscopy. Scanning electron micrographs of our sHz shows that they are homogeneous in size and shape (Fig. S1b). Synthetic Hz failed to induce proinflammatory cytokines such as TNFα (Fig. S1c), consistent with data from other groups (Dostert et al., 2009; Griffith et al., 2009; Parroche et al., 2007; Reimer et al., 2010).

We found that Hz-laden CpG DNA (sHz/CpG) was rapidly internalized into the phagolysosome of bone marrow derived macrophages (BMDMs), along with its Alexa647-labeled DNA cargo (Fig. 1b, top). Although free CpG DNA engages TLR9 in the early endosomal compartment, Rab 4 (an early endosomal marker) did not co-localize with sHz (Fig. 1b, bottom). In order to determine if this is relevant to what occurs *in vivo*, we incubated BMDMs with *Plasmodium* infected RBCs (iRBCs) from mice that were injected with BrdU. As shown in Fig. 1c, by 1h, iRBCs were engufed into the phagolysosome where nHz was observed together with fluorescently labeled plasmodial DNA (Fig. 1d, middle). However, by the 12h time point, Hz and DNA dissociated (Fig. 1d, bottom) and no longer appeared to be within the phagosome.

The activity of the inflammasome is commonly broken down into a “priming” step and a second step that results in the assembly of a larger complex that generates mature cytokines. We used a macrophage cell line that expresses ectopic ASC-CFP to examine the kinetics of inflammasome activation by Hz (Bauernfeind et al., 2009). Inflammasome assembly was visualized in ~ 40% of the macrophages that were exposed to sHz/CpG within 6 h of incubation (Fig. 1e and S1d). In addition, sHz/CpG provided all of the necessary signals to result in the production of mature IL-1β (Figs. 1f and S1e), in contrast to sHz or CpG DNA alone. In order to determine which inflammasome was being activated, cell lines derived from several knockout mice were analyzed. This experiment (Fig. 1g), confirmed the observations of several other groups that the second signal in NLRP3 inflammasome activation could be provided by sHz (Dostert et al., 2009; Griffith et al., 2009; Reimer et al., 2010; Shio et al., 2009). These results were confirmed in primary wild type (wt) and *Nlrp3* deficient macrophages (S1f). Although these experiments were performed using the mouse CpG oligonucleotide (ODN) known as 1826, we observed similar results with CpG ODNs derived from the genome of *Pf* (S1g). In contrast to NLRP3, NLRP6 (Elinav et al., 2011) and NLRP12 (Arthur et al., 2010) were dispensable for sHz/CpG-mediated IL-1β release (Fig. S1h).

Hz traffics *Pf* gDNA into the lysosomal compartment, resulting in accessibility to TLR9

Confocal imaging of sHz/CpG within macrophages revealed that over time, DNA bound to Hz dissociated from the crystal (Fig. 2a and Fig. 1d, bottom) and that Hz mediated a loss of

phagolysosomal integrity. Surprisingly, as the phagolysosome disintegrated, the crystal appears to have been released, while the CpG DNA remained bound to the lysosomal compartment, as defined by staining with lysosotracker (Fig. 2b). Since lysotracker selectively stains all acidic compartments, we also used lamp1-Kate2 macrophages (which express fluorescent lamp1) and obtained similar results (Fig. S2a and Fig. 5f). We hypothesized that the reason CpG DNA remained with the phagolysosome was that it was bound to endosomal TLRs, such as TLRs 3, 7 and 9. When the same experiment was performed with macrophages from Unc93b mutant mice, which fail to translocate TLR3, TLR7 and TLR9 to the lysosomal compartment (Tabeta et al., 2006), DNA dissociated from the sHz and transited to the cytosol (Fig. 2c).

We have previously hypothesized that Hz traffics DNA into a lysosomal compartment where it could engage TLR9 (Parroche et al., 2007). We used BMDMs from a transgenic mouse that expresses GFP-tagged TLR9 (Fig. 2d) to directly test our hypothesis. When exposed to sHz, TLR9 remained in the endoplasmic reticulum. When fluorescently labeled free CpG ODN were internalized into the endolysosomal compartment, TLR9 almost completely co-localized with the ODN within 30 minutes, as expected (Latz et al., 2004). Similarly, sHz/CpG was internalized rapidly into phagosomes, and provided the necessary signals for TLR9 translocation. Synthetic Hz that was coated with *Pf* gDNA resulted in the movement of TLR9 to the phagolysosome, similar to sHz/CpG (Fig. 2d).

The translocation of TLR9 to the phagosome plays a critical role in priming the NLRP3 inflammasome. While sHz/CpG and sHz/*Pf* gDNA were sufficient to induce the production and secretion of active IL-1β, this did not occur in macrophages from *Tlr9*−/− mice (Fig. 2e). Indeed, a true physiologic role for TLR9 in IL-1β production is suggested by the finding that sHz/*Pf* gDNA and sHz/CpG were nearly identical in dependence on TLR9 expression in order to induce the secretion of IL-1β (Fig. 2e).

Although sHz interacts weakly with *Pf* gDNA (Jaramillo et al., 2009) it has been shown that host and plasmodial proteins interact with the Hz crystal (Ashong et al., 1989; Goldie et al., 1990; Jaramillo et al., 2009). Accordingly, we coated sHz with Fetal Bovine Serum (FBS) and then incubated the protein-coated sHz with *Pf* gDNA. In contrast to “naked” sHz, serum-coated sHz interacted strongly with *Pf* gDNA (Fig. S2b). These findings imply that proteins bind to nHz and form a bridge with *Pf* gDNA during infection. Indeed, several years ago, we found that proteinase K treated nHz lost its DNA coating (data not shown). Taken together, these findings may explain an observation made almost 20 years ago by Pichyangkul *et al*., who reported that protease-treated nHz lost its ability to induce TNFα and IL-1β from human monocytes (Pichyangkul et al., 1994); protease treatment undoubtedly removed the surface DNA from nHz that was responsible for cytokine induction.

NLRP3 activation by Hz requires phagocytosis of the crystals and leads to phagolysosomal destabilization

As can be seen in Fig. 3a, the inhibition of crystal engulfment by cytochalasin D resulted in dose-dependent disruption of NLRP3 activity as evidenced by the inhibition of IL-1β production in macrophages exposed to sHz-complexed with CpG DNA (Fig. 3b).

Cytochalasin D had no effect on the release of IL-1β upon stimulation with potassium ionophore nigericin (Fig. 3b).

Similar to sHz, macrophages actively engulf nHz crystals. Within a few hours of phagocytosis, nHz induced phagolysosomal instability. For example, as shown in Fig. 3c, one can see that untreated macrophages accumulate fluorescent dextran in lysosomes, and form a punctate staining pattern. In contrast, macrophages that have engulfed nHz no longer accumulate fluorescent dextran in their lysosomal compartment due to the loss of phagolysosomal integrity. These data have been repeated with sHz with similar results (Fig. S3a). To further evaluate the effect of Hz on the shape and size of lysosomes, we stained macrophages with acridine orange. This dye binds to both DNA and RNA in the nucleus and cytosol, where it fluoresces green (525 nm). As seen in Fig. 3d, acridine orange becomes highly concentrated in the lysosomal compartment under acidic conditions and fluoresces red (600–650 nm) (Hornung et al., 2008). The loss of phagolysosomal integrity was quantified by flow cytometry, where there is dose dependent loss of red fluorescence, as acridine orange escaped to the cytosol (Fig. 3e). Note that the data shown in Figs 3d and 3e have also been repeated with sHz with similar results (data not shown). Taken together, these results indicate that phagocytosis of Hz crystals leads to the loss of phagolysosomal integrity, resulting in the leakage of the lysosomal contents into the cytosol.

We next tested the effects of bafilomycin A, an H+ ATPase inhibitor that leads to the neutralization of lysosomal pH and prevents the activation of most lysosomal proteases, including cathepsins. Bafilomycin A significantly blocked the sHz/CpG mediated release of IL-1β but had no effect on nigericin (Fig. 3f). These data suggest that lysosomal acidification is critical in sHz/CpG mediated inflammasome activation. When bafilomycin A was added to cells before their exposure to sHz, the phagolysosome did not remain intact suggesting that phagolysosomal integrity is independent of lysosomal pH (data not shown). Several cathepsins, including cathepsin B and L, have been reported as important in mediating inflammasome activation in response to crystal exposure (Duewell et al., 2010; Hornung et al., 2008). Immortalized BMDMs from *Ctsb*$^{-/-}$ and *Ctsl*$^{-/-}$ mice had reduced levels of IL-1β after sHz/CpG exposure (Fig. 3g). Similarly, specific inhibitors of various cathepsins inhibited IL-1β release (Fig. S3b). These data suggest that the cathepsins might play a role in Hz- mediated inflammasome activation.

A number of studies have demonstrated a role for uric acid in the immune response to malaria (Guermonprez et al., 2013; Lopera-Mesa et al., 2012; Orengo et al., 2008; Orengo et al., 2009; van de Hoef et al., 2013) and released urate has been suggested as the cause of Hz-induced inflammasome activation *in vivo* (Griffith et al., 2009). To determine if sHz is activating NLRP3 via the release of uric acid, we pretreated macrophages with uricase before adding sHz/CpG. Uricase added to the monosodium urate stimulated cells resulted in a dose dependent decrease in IL-1β release while it had no effect on the response to sHz/CpG treated cells (Fig. 3h). Hence, sHz did not appear to be activating NLRP3 through the release of uric acid.

Plasmodial gDNA on the surface of Hz induces mature IL-1β production in macrophages through the AIM2 inflammasome

Genomic *Pf* DNA, when transfected into LPS-primed macrophages, induced IL-1β release (Fig. 4a). IL-1β production was independent of NLRP3 expression, but dependent on ASC and caspase-1, indicating that parasite gDNA is recognized by an alternative inflammasome (Fig. 4a). AIM2 is a HIN-200 family member that directly binds cytosolic double stranded DNA, resulting in the formation of inflammasomes. We transfected *Pf* gDNA into the cytosol of *Aim2*$^{+/+}$ and *Aim2*$^{-/-}$ primary macrophages, and discovered that AIM2 expression was essential for IL-1β production, regardless of the strain of *Pf* from which the gDNA was obtained (Fig. 4b). The results of these functional assays were confirmed when cells were analyzed by confocal microscopy. ASC-CFP speck formation was activated by transfection of *Pf* gDNA; indeed, the gDNA co-localized with the developing ASC pyroptosome (Fig. 4c and Fig. S4a), consistent with the prediction that the DNA is binding directly to AIM2. In support of this hypothesis, we transfected *Pf* gDNA into macrophages that express AIM2-citrine. Speck formation was again observed, and AIM2 co-localized with the DNA (Fig. 4d and Fig. S4b). Incubating these cells with sHz/*Pf* gDNA induced AIM2 pyroptosome formation (Fig. S4c), while sHz alone (Fig. 4d, bottom panel) did not induce AIM2 pyroptosome formation in AIM2-citrine cells. Conversely, transfection of *Pf* gDNA into cells that expressed fluorescently tagged NLRP3 (Bauernfeind et al., 2009) did not result in speck formation (Fig. 4e). On the other hand, when *Pf* gDNA was introduced into unprimed cells on the surface of sHz via a phagocytic pathway, NLRP3 pyroptosome formation was observed (Fig. 4e and Fig. S4d). These observations are consistent with the concept that when innate immune cells are exposed to sHz/DNA, the DNA can prime the macrophages via TLR9 in the phagosome, generating NLRP3 and pro-IL-1β; DNA subsequently directly activates the AIM2 inflammasome once it has access to the cytosol. The role of Hz, with respect to AIM2, is to allow DNA that enters cells via a phagocytic pathway access to the cytosol.

Natural Hz induces IL-1β release through the activation of both NLRP3 and AIM2

During the *Plasmodium* life cycle, merozoites containing Hz, as well as free Hz, are released into the blood stream upon schizont rupture. During this process, parasites and their products are rapidly internalized by phagocytes, especially those that reside in the liver and spleen. In turn, these cells produce cytokines, chemokines and other immunomodulators. Synthetic Hz complexed to CpG DNA triggers the inflammasome pathway, providing both an NF-κB signal to induce NLR and pro-IL-1β expression and a second signal to induce inflammasome assembly. We purified nHz from cultures of *Pf* and used that to stimulate cells in order to validate sHz/CpG as a model of natural Hz crystal.

Examination of nHz by microscopy confirmed that it was free of contaminating iRBC or parasites. As shown in Fig. 5a and Fig. S5a, nHz caused the formation of ASC specks in immortalized BMDMs. In addition, nHz induced IL-1β release from primary C57Bl/6 macrophages (Fig. 5b, top left panel). This ability of nHz to induce IL-1β from BMDMs was dramatically diminished, but not abolished, when nHz was used to stimulate BMDMs from *Nlrp3*$^{-/-}$ mice (Fig. 5b, top right). Similarly, BMDMs from *Aim2*$^{+/+}$ mice were highly responsive to nHz (Fig. 5b, lower left), but responses were greatly diminished, but not

abolished, in cells from *AIM2*$^{-/-}$ mice (Fig. 5b, lower middle). When we crossed the *Aim2* knockout with the *Nlrp3* knockout mouse (*Aim2*$^{-/-}$*Nlrp3*$^{-/-}$), we found that the residual IL-1β inducing activity was gone (Fig. 5b, lower right).

In addition to the ability of nHz to induce IL-1β production, we evaluated cell viability using the vital probe calcein AM. Natural Hz-induced inflammasome activation resulted in pyroptotic cell death in a dose-dependent manner in wt macrophages, but caused significantly less cell death in ASC and caspase-1 deficient macrophages. *Nlrp3* deficient macrophages were partly resistant to cell death (Fig. S5b and S5c). We also incubated *Aim2*$^{+/+}$, *Aim2*$^{-/-}$ and *Nlrp3*$^{-/-}$*Aim2*$^{-/-}$ double knockout BMDMs with nHz. Natural Hz induced cell death in *Aim2*$^{+/+}$ BMDMs but was rescued partly in *Aim2*$^{-/-}$ and almost completely in *Nlrp3*$^{-/-}$*Aim2*$^{-/-}$ double knockout BMDMs (Fig. 5c), suggesting that NLRP3 and AIM2 inflammasomes together mediate most of the nHz-induced cell death in macrophages.

These observations were confirmed by western blots of livers harvested from animals injected with sHz/*Pf* gDNA. It should be noted that mammalian livers have a large quantity of preformed pro-IL-1β, presumably because the liver is constantly being primed by bacterial products absorbed from the gastrointestinal track. After injection with sHz/gDNA, the mature 17kDa IL-1β was significantly reduced in the *Nlrp3*$^{-/-}$*Aim2*$^{-/-}$ *d*ouble knockout mice compared to littermate controls (Fig. 5d and original blots in Fig. S5d). Hence, sHz/*Pf* gDNA activates both the AIM2 and the NLRP3 inflammasomes.

Our *in vitro* results presented above revealed the potent capability of nHz to induce pro-inflammatory responses via NLRP3 and AIM2 inflammasomes. To confirm the physiological relevance of this *in vivo*, in the context of Hz-induced inflammation, we used a peritonitis model. Mice were injected intraperitoneally with sHz/*Pf* gDNA. The sHz/*Pf* gDNA induced a considerable increase in the recruitment of neutrophils to the peritoneal cavity in wt but not in *Nlrp3*$^{-/-}$, *Aim2*$^{-/-}$ *and Nlrp3*$^{-/-}$*Aim2*$^{-/-}$ double knockout mice (Fig. 5e).

Overall, the data suggest that the initial signals necessary for the synthesis of pro-IL-1β are through DNA activation of TLR9. In addition, inflammasome assembly and activation seems to be due to the loss of phagolysosomal integrity that both allows for the assembly of NLRP3 while facilitating the direct binding of double stranded *Pf* gDNA to AIM2. This model of innate immune activation is predicated on the belief that DNA dissociates from Hz in the phagolysosome and ultimately gains access to the cytosol. In fact, this is what was observed: genomic DNA from *Plasmodium* was stained with DAPI, and bound overnight to serum-coated sHz. These sHz/*Pf* gDNA complexes were fed to macrophages and followed by confocal microscopy over time. As seen in Fig. 5f, both free DNA and Hz could be found outside the lysosomal compartment. This result confirms that Hz is responsible for delivering DNA to the cytosol, where DNA can activate cytosolic DNA receptors. I`n addition to AIM2, cytosolic DNA sensors can also trigger the production of Type I interferons under these conditions.

Plasmodium-infected erythrocytes induce IL-1β production via both the NLRP3 and AIM2 inflammasomes similar to DNA-coated sHz

Peripheral smears of patients with high parasitemia malaria often reveal the presence of Hz in phagocytes. This Hz is presumably due to the phagocytosis and degradation of parasites that contained Hz (Bettiol et al., 2010; Ing et al., 2006; McGilvray et al., 2000) in addition to the uptake of any free Hz that may be in the vasculature. *Plasmodium berghei* infected RBCs (iRBCs) often have visible Hz within them when stained with Giemsa. If Hz that is present in iRBCs is truly a major immune activator, we hypothesized that the innate immune activating activity of phagocytosed iRBCs should resemble that of purified nHz or sHz that is experimentally coated with plasmodial gDNA.

To visualize the uptake of iRBCs by macrophages, we fed macrophages RBCs infected with fluorescent *P. berghei* NK65 (Fig. 6a). These iRBCs were fully competent to activate IL-1β production from unprimed macrophages (Fig. 6b). As was the case with sHz/CpG (Fig. 3f), this process was inhibited by blocking phagolysosomal acidification with bafilomycin A (Fig. 6b). Hz could be seen within phagocytosed *P. berghei*-infected RBCs and induced phagolysosomal destabilization (Fig. S6a). Like sHz/CpG or nHz (Fig. 1e and Fig. 5a, respectively), iRBC triggered the formation of ASC specks in the cytosol of ASC-CFP macrophages (Fig. 6c and Fig. S6b). Uninfected RBCs (uRBC)s did not induce the formation of ASC-pyroptosomes (data not shown). Similar to sHz/gDNA and nHz, AIM2 activation by *P. berghei*-infected RBCs was observed when examined by the speck assay. When we pre-stained parasites with the nucleic acid stain DAPI, and then co-cultured iRBCs with AIM2-citrine macrophages, AIM2 assembly was observed. In fact, DAPI-stained DNA actually co-localized with the AIM2 inflammasome (Fig. 6d, bottom panel and Fig. S6c).

We next exposed wild-type and TLR9 knockout macrophages to infected RBC and measured IL-1β production. Wild-type BMDMs responded robustly to infected RBC in the absence of a priming step. The priming step, in fact, appeared to be TLR9 dependent (Fig. 6e) and iRBCs induced TLR9 translocation (data not shown). When macrophages from *Nlrp3*$^{-/-}$ (Fig. 6f, upper right panel) and *Aim2*$^{-/-}$ (Fig. 6f, lower middle panel) mice were tested, we observed a markedly decreased response compared to their littermate controls. No response was observed in the *Nlrp3*$^{-/-}$*Aim2*$^{-/-}$ double knockout cells (Fig. 6f, lower right panel). Hence, the characteristics of macrophage stimulation by infected erythrocytes resembled, in all respects, that of *Pf* gDNA-coated sHz or nHz.

DISCUSSION

Malaria remains one of the most important infectious diseases in the world today. The disease is typically characterized by recurrent febrile paroxysms that are attributed to circulating pro-inflammatory cytokines released in response to the parasite components (Adachi et al., 2001; Pichyangkul et al., 1994; Sherry et al., 1995; Taramelli et al., 1998). Malaria is a complicated disease in which many parasite and host components contribute to disease severity. Nevertheless, understanding the details of the innate host response is truly important because the details of the cytokine response have the potential to lead to translational breakthroughs. The current data set, for example, raises the possibility that immunomodulation of the NLRP3 and AIM2 inflammasomes activity might be therapeutic.

As we learn more about inflammation in malaria, Hz has surprisingly emerged as a key component of almost every aspect of innate immune activation. We have previously suggested that Hz acts as a delivery agent, introducing DNA into the lysosomal compartment. Yet, as we have shown here, Hz does much more than help DNA engage TLR9 as it is essential for activation of NLRP3, AIM2 and even (by extrapolation) the type I interferon response that occurs in the cytosol of immune cells. This overall scheme of innate immune activation in malaria is diagrammed in Fig. S6d.

One question that requires more mechanistic study is how DNA might actually co loacalize with Hz in infected erythorocytes considering that Hz is normally in the food vacuole of the parasite. One possibility is that during the process of parasite expansion, there is constant turnover of a subpopulation of parasites, and that during this process of parasite turnover, Hz may be exposed to parasite DNA. Indeed, a recent paper by Greenbaum and colleagues (Love et al., 2012), provides evidence that this occurs as the result of human platelet factor 4, which kills plasmodium inside erythrocytes by selectively lysing the parasite digestive vacuole, ultimately killing the parasite. As the parasite nucleus undergoes karyolysis, it is clear plasmodial DNA and Hz can mix in the cytosol.

As confirmed here, Hz is a potent activator of the NLRP3 inflammasome (Dostert et al., 2009; Griffith et al., 2009; Reimer et al., 2010; Shio et al., 2009). As the NLRP3 inflammasome is a potential source of large quantities of mature IL-1β, this role of Hz must be considered to be quite important. Indeed, along with TNFα, IL-1β has been recognized as one of the cytokines most closely associated with death during malaria (Day et al., 1999; Kwiatkowski et al., 1990; Prakash et al., 2006; Vogetseder et al., 2004). The pleitropic effects of IL-1β might explain some discrepancies between our results and those of Jaramillo *et al*. (Jaramillo et al., 2009) especially *in vivo*, where sHz would be expected to induce the production of IL-1β (and IL-18) from the liver in the absence of priming. Perhaps even more important than the role of Hz in activating the NLRP3 inflammasome, Hz has a destabilizing activity on the integrity of the phagolysosome. The result of this activity is to allow phagolysosomal components access to the cytosol. The integrity of the cytosol is of paramount importance to immune cells, and the subsequent widespread activation of the innate immune system is not surprising.

Natural Hz contains abundant proteins associated with the crystal (Ashong et al., 1989; Goldie et al., 1990) and the effects of these proteins remain to be fully defined. The present report does not rule out an important role for these proteins, as the work was relatively narrow in its focus on DNA. For example, it has been reported that host serum fibrinogen, which is stably bound to Hz, strongly increases the capacity of nHz to activate monocyte inflammatory functions (Barrera et al., 2011). Indeed, Hz, DNA and host associated proteins could potentially form a complex and augment innate immune responses.

The demonstration of innate immune activation in human patients lags far behind what we have learned from *in vitro* modeling of the innate immune response in tissue culture, and *in vivo* modeling in rodents. Close biochemical and immunological studies of innate immune responses in patients are complicated by the inaccessibility of certain important tissues (*e.g.*, human spleens, livers and brains) that obviously cannot be harvested during the course of

illness. Hence, we are reliant upon mouse models and the examination of peripheral cells to make educated guesses about what is happening in severe disease. This is an important effort, because if the world is to develop effective immunomodulatory remedies for life-threatening disease, as well as a truly effective malaria vaccine, dramatic improvements in our understanding of biology of inflammation during malaria are necessary.

Experimental Procedures

Mice

C57BL/6, *Nlrp3*$^{-/-}$, *Nlrp6*$^{-/-}$ and *Nlrp12*$^{-/-}$ mice were purchased from Jackson Laboratories. *Asc*$^{-/-}$ (Pycard$^{-/-}$) mice were provided by Millennium Pharmaceuticals. Caspase-1 deficient mice (*Casp1*$^{-/-}$) were provided by A. Hise (Case Western Reserve), *Ctsb*$^{-/-}$ by T. Reinheckel (University of Freiburg) and *Ctsl*$^{-/-}$ by H. Ploegh (MIT). *Aim2*$^{+/+}$ and *Aim2*$^{-/-}$ were generated as described in Ref. (Rathinam et al., 2010), *Tlr9*$^{-/-}$ mice were a gift of S. Akira (Osaka Univesrity). UNC93B1 mutant (3d) mice were from by B. Beutler (University of Texas Southwestern). Mice 6–8 weeks of age were used in all experiments. All mouse strains were bred and maintained under specific pathogen-free conditions at the University of Massachusetts Medical School.

Reagents

Lipofectamine 2000 was from Invitrogen (Carlsbad, CA). Poly (dAdT), Cytochalasin D and Pepstain A, acridine orange and bromodeoxyuridine were from Sigma-Aldrich. Bafilomycin A1 and giemsa stain were from Fluka Analytical. Alexa Fluor 546-conjugated dextran, Lysotracker, Cell Mask Plasma membrane stain, DAPI, SYTO 60, Calcein AM and propidium iodide were from Molecular Probes/Invitrogen (Carlsbad, CA). Nigericin was from Invivogen; CA-074Me was from Enzo LifeSciences; Cat L inhibitor was from Calbiochem; uricase (Elitek) was from Sanofi-Aventis. DMEM medium was from Cellgro (Manassas, VA) and low endotoxin FBS was from Atlas Biologicals (Fort Collins, CO). CpG DNA oligodeoxynucleotide 1826 and CpG-Alexa 647 and AT2-A647 were obtained from IDT (Coralville, IA). *Pf* 3D7 genomic DNA was purified as described (Parroche et al., 2007). *Pf* HB3_B2, *Pf* T9/94 and *Pf* Dd2 genomic DNA were obtained from the malaria research and reference resource center at NIAID.

Confocal microscopy and flow cytometry

Confocal reflection microscopy was combined with fluorescence microscopy as described in (Hornung et al., 2008) on a Leica TCS SP8 AOBS confocal laser-scanning microscope. Flow cytometry was performed as described in (Hornung et al., 2008).

Cell culture, stimulations, ELISA and immunoblot analysis

Immortalized macrophage cell lines were generated from wt, *NLRP3*$^{-/-}$, *ASC*$^{-/-}$, *caspase1*$^{-/-}$, *TLR9*$^{-/-}$, *ctsb*$^{-/-}$, *ctsl*$^{-/-}$ and 3d mice (Hornung et al., 2008). Primary BMDMs were generated as described (Rathinam et al., 2010). Human PBMCs were isolated from whole blood of healthy volunteers by density gradient centrifugation. All cells, primary and cell lines were cultured in DMEM supplemented with Ciprofloxacin and 10% FBS. For all experiments for immunoblot analysis, serum-free DMEM medium was used. For

stimulations, poly (dAdT) (1.5 μg/ml) or genomic DNA was transfected with lipofectamine 2000 (Invitrogen). Nigericin (10 μM) was added 1 h before supernatants were collected. 2×10^5 macrophages were plated and stimulated the day after with indicated amounts of CpG, sHz, nHz, sHz/CpG and sHz/*Pf* gDNA, iRBCs and RBCs. Cytokine measurements were performed using ELISA kits for mouse IL-1β and TNFα (R&D systems). Immunoblot analysis was performed with anti– mouse IL-1β antibody (AF-401-NA; R&D Systems) and rabbit anti-goat IgG-HRP (Santa Cruz Biotechnology).

Culture of parasites, preparation of sHz and nHz, preparation of sHz/CpG and sHz/*Pf* gDNA

Synthetic Hz was prepared using hemin chloride (Sigma, > 98% HPLC) as previously described (Shio et al., 2009). The dried pigment was suspended in endotoxin-free PBS (Cellgro, Manassas, VA) and inspected by microscopy for size and other characteristics; the crystalline nature of the crystals was confirmed by reflection confocal microscopy and electron microscopy (Fig. S1b). *Pf* parasites (3D7 strain) were cultured as previously described (Parroche et al., 2007). *Pf* culture stages and parasitemia levels were assessed daily by Giemsa staining and also checked routinely for Mycoplasma. Natural Hz was extracted from the parasite cultures as described in (Parroche et al., 2007). The dried pigment was suspended in endotoxin-free PBS and stored at 4°C. Synthetic Hz/CpG complexes were prepared by incubating sHz and CpG in a rocker for 2 h and washing the complex three times with PBS. Synthetic Hz/*Pf* gDNA was prepared by coating sHz with FBS (Atlas Biologicals) overnight and then incubating with *Pf* gDNA for 2 h followed by three washes with PBS.

Infection of mice

Plasmodium berghei (NK65) Red star, *Plasmodium berghei* (Pb) NK65 and *Plasmodium berghei* (Pb) ANKA were obtained from the malaria research and reference resource center (MR4) and maintained by passage in BALB/c mice. Parasitemia level was assessed every 3 days by microscopic examination of Giemsa-stained smears of blood.

In vivo labeling of *Plasmodium* with BrdU

C57BL/6 mice infected with *Plasmodium berghei* ANKA were injected daily intraperitoneally with 1mg of BrdU in 1 ml of PBS on days 9, 10 and 11 post-infection. Blood was harvested by cardiac puncture on day 12. Blood was washed several times and 1ml of mouse blood was layered onto 1ml of MonoPoly Resolving Medium and centrifuged for 45 min at 3000 rpm. After centrifugation, RBCs in the bottom layer were collected, washed and resuspended in PBS. RBC suspensions were subsequently loaded into an LS column (Miltenyi Biotec, Auburn, CA) and placed into a MACS separator. The flow through (devoid of free Hz) was collected and loaded onto an LD column (Miltenyi Biotec, Auburn, CA). When removed from the magnetic field, the subsequent flow through contained ~ 99% *Plasmodium* infected erythrocytes. BMDMs were incubated with iRBCs for various time periods, fixed using ice-cold 70% ethanol and then incubated with 2M HCl for 30 min at room temperature. Cells were washed 2 times with PBS, incubated with FITC-conjugated anti-BrdU antibody (eBiosciences) for 2 h in the dark and subjected to confocal microscopy.

Supplementary Material

Refer to Web version on PubMed Central for supplementary material.

Acknowledgments

The authors would like to thank Anna Cerny for animal husbandry. We thank Drs. Shizuo Akira, Bruce Beutler and Hidde Pleogh (Massachusetts Institutes of Technology, Boston) for their transgenic mice. This work is supported by NIH grants AI067497 (to K.A.F) and by AI079293 (to K.A.F and D.T.G), by R21AI80907 (to R.T.G.).

REFERENCES

Adachi K, Tsutsui H, Kashiwamura S, Seki E, Nakano H, Takeuchi O, Takeda K, Okumura K, Van Kaer L, Okamura H, et al. Plasmodium berghei infection in mice induces liver injury by an IL-12- and toll-like receptor/myeloid differentiation factor 88-dependent mechanism. J Immunol. 2001; 167:5928–5934. [PubMed: 11698470]

Arthur JC, Lich JD, Ye Z, Allen IC, Gris D, Wilson JE, Schneider M, Roney KE, O'Connor BP, Moore CB, et al. Cutting edge: NLRP12 controls dendritic and myeloid cell migration to affect contact hypersensitivity. J Immunol. 185:4515–4519. [PubMed: 20861349]

Arthur JC, Lich JD, Ye Z, Allen IC, Gris D, Wilson JE, Schneider M, Roney KE, O'Connor BP, Moore CB, et al. Cutting edge: NLRP12 controls dendritic and myeloid cell migration to affect contact hypersensitivity. J Immunol. 2010; 185:4515–4519. [PubMed: 20861349]

Ashong JO, Blench IP, Warhurst DC. The composition of haemozoin from Plasmodium falciparum. Trans R Soc Trop Med Hyg. 1989; 83:167–172. [PubMed: 2692224]

Barrera V, Skorokhod OA, Baci D, Gremo G, Arese P, Schwarzer E. Host fibrinogen stably bound to hemozoin rapidly activates monocytes via TLR-4 and CD11b/CD18-integrin: a new paradigm of hemozoin action. Blood. 2011; 117:5674–5682. [PubMed: 21460246]

Bauernfeind FG, Horvath G, Stutz A, Alnemri ES, MacDonald K, Speert D, Fernandes-Alnemri T, Wu J, Monks BG, Fitzgerald KA, et al. Cutting edge: NF-kappaB activating pattern recognition and cytokine receptors license NLRP3 inflammasome activation by regulating NLRP3 expression. J Immunol. 2009; 183:787–791. [PubMed: 19570822]

Bettiol E, Van de Hoef DL, Carapau D, Rodriguez A. Efficient phagosomal maturation and degradation of Plasmodium-infected erythrocytes by dendritic cells and macrophages. Parasite Immunol. 32:389–398. [PubMed: 20500669]

Bettiol E, Van de Hoef DL, Carapau D, Rodriguez A. Efficient phagosomal maturation and degradation of Plasmodium-infected erythrocytes by dendritic cells and macrophages. Parasite Immunol. 2010; 32:389–398. [PubMed: 20500669]

Brown H, Turner G, Rogerson S, Tembo M, Mwenechanya J, Molyneux M, Taylor T. Cytokine expression in the brain in human cerebral malaria. J Infect Dis. 1999; 180:1742–1746. [PubMed: 10515846]

Burckstummer T, Baumann C, Bluml S, Dixit E, Durnberger G, Jahn H, Planyavsky M, Bilban M, Colinge J, Bennett KL, et al. An orthogonal proteomic-genomic screen identifies AIM2 as a cytoplasmic DNA sensor for the inflammasome. Nat Immunol. 2009; 10:266–272. [PubMed: 19158679]

Clark IA, Cowden WB, Rockett KA. The pathogenesis of human cerebral malaria. Parasitol Today. 1994; 10:417–418. [PubMed: 15275522]

Clark IA, Rockett KA. The cytokine theory of human cerebral malaria. Parasitol Today. 1994; 10:410–412. [PubMed: 15275552]

Coban C, Ishii KJ, Kawai T, Hemmi H, Sato S, Uematsu S, Yamamoto M, Takeuchi O, Itagaki S, Kumar N, et al. Toll-like receptor 9 mediates innate immune activation by the malaria pigment hemozoin. J Exp Med. 2005; 201:19–25. [PubMed: 15630134]

Day NP, Hien TT, Schollaardt T, Loc PP, Chuong LV, Chau TT, Mai NT, Phu NH, Sinh DX, White NJ, et al. The prognostic and pathophysiologic role of pro- and antiinflammatory cytokines in severe malaria. J Infect Dis. 1999; 180:1288–1297. [PubMed: 10479160]

Dostert C, Guarda G, Romero JF, Menu P, Gross O, Tardivel A, Suva ML, Stehle JC, Kopf M, Stamenkovic I, et al. Malarial hemozoin is a Nalp3 inflammasome activating danger signal. PLoS One. 2009; 4:e6510. [PubMed: 19652710]

Duewell P, Kono H, Rayner KJ, Sirois CM, Vladimer G, Bauernfeind FG, Abela GS, Franchi L, Nunez G, Schnurr M, et al. NLRP3 inflammasomes are required for atherogenesis and activated by cholesterol crystals. Nature. 2010; 464:1357–1361. [PubMed: 20428172]

Elinav E, Strowig T, Kau AL, Henao-Mejia J, Thaiss CA, Booth CJ, Peaper DR, Bertin J, Eisenbarth SC, Gordon JI, et al. NLRP6 inflammasome regulates colonic microbial ecology and risk for colitis. Cell. 2011; 145:745–757. [PubMed: 21565393]

Franklin BS, Parroche P, Ataide MA, Lauw F, Ropert C, de Oliveira RB, Pereira D, Tada MS, Nogueira P, da Silva LH, et al. Malaria primes the innate immune response due to interferon-gamma induced enhancement of toll-like receptor expression and function. Proc Natl Acad Sci U S A. 2009; 106:5789–5794. [PubMed: 19297619]

Gardner MJ, Hall N, Fung E, White O, Berriman M, Hyman RW, Carlton JM, Pain A, Nelson KE, Bowman S, et al. Genome sequence of the human malaria parasite Plasmodium falciparum. Nature. 2002; 419:498–511. [PubMed: 12368864]

Gazzinelli RT, Denkers EY. Protozoan encounters with Toll-like receptor signalling pathways: implications for host parasitism. Nat Rev Immunol. 2006; 6:895–906. [PubMed: 17110955]

Goldie P, Roth EF Jr, Oppenheim J, Vanderberg JP. Biochemical characterization of Plasmodium falciparum hemozoin. Am J Trop Med Hyg. 1990; 43:584–596. [PubMed: 2267961]

Gowda NM, Wu X, Gowda DC. The Nucleosome (Histone-DNA Complex) Is the TLR9-Specific Immunostimulatory Component of Plasmodium falciparum That Activates DCs. PLoS One. 2011; 6:e20398. [PubMed: 21687712]

Grau GE, Heremans H, Piguet PF, Pointaire P, Lambert PH, Billiau A, Vassalli P. Monoclonal antibody against interferon gamma can prevent experimental cerebral malaria and its associated overproduction of tumor necrosis factor. Proc Natl Acad Sci U S A. 1989; 86:5572–5574. [PubMed: 2501793]

Griffith JW, Sun T, McIntosh MT, Bucala R. Pure Hemozoin is inflammatory in vivo and activates the NALP3 inflammasome via release of uric acid. J Immunol. 2009; 183:5208–5220. [PubMed: 19783673]

Guermonprez P, Helft J, Claser C, Deroubaix S, Karanje H, Gazumyan A, Darasse-Jeze G, Telerman SB, Breton G, Schreiber HA, et al. Inflammatory Flt3l is essential to mobilize dendritic cells and for T cell responses during Plasmodium infection. Nat Med. 2013; 19:730–738. [PubMed: 23685841]

Halle A, Hornung V, Petzold GC, Stewart CR, Monks BG, Reinheckel T, Fitzgerald KA, Latz E, Moore KJ, Golenbock DT. The NALP3 inflammasome is involved in the innate immune response to amyloid-beta. Nat Immunol. 2008; 9:857–865. [PubMed: 18604209]

Hornung V, Ablasser A, Charrel-Dennis M, Bauernfeind F, Horvath G, Caffrey DR, Latz E, Fitzgerald KA. AIM2 recognizes cytosolic dsDNA and forms a caspase-1-activating inflammasome with ASC. Nature. 2009; 458:514–518. [PubMed: 19158675]

Hornung V, Bauernfeind F, Halle A, Samstad EO, Kono H, Rock KL, Fitzgerald KA, Latz E. Silica crystals and aluminum salts activate the NALP3 inflammasome through phagosomal destabilization. Nat Immunol. 2008; 9:847–856. [PubMed: 18604214]

Ing R, Segura M, Thawani N, Tam M, Stevenson MM. Interaction of mouse dendritic cells and malaria-infected erythrocytes: uptake, maturation, and antigen presentation. J Immunol. 2006; 176:441–450. [PubMed: 16365437]

Jaramillo M, Bellemare MJ, Martel C, Shio MT, Contreras AP, Godbout M, Roger M, Gaudreault E, Gosselin J, Bohle DS, et al. Synthetic Plasmodium-like hemozoin activates the immune response: a morphology - function study. PLoS One. 2009; 4:e6957. [PubMed: 19742308]

Jaramillo M, Godbout M, Olivier M. Hemozoin induces macrophage chemokine expression through oxidative stress-dependent and -independent mechanisms. J Immunol. 2005; 174:475–484. [PubMed: 15611273]

Kwiatkowski D, Hill AV, Sambou I, Twumasi P, Castracane J, Manogue KR, Cerami A, Brewster DR, Greenwood BM. TNF concentration in fatal cerebral, non-fatal cerebral, and uncomplicated Plasmodium falciparum malaria. Lancet. 1990; 336:1201–1204. [PubMed: 1978068]

Kwiatkowski D, Nowak M. Periodic and chaotic host-parasite interactions in human malaria. Proc Natl Acad Sci U S A. 1991; 88:5111–5113. [PubMed: 2052590]

Last-Barney K, Homon CA, Faanes RB, Merluzzi VJ. Synergistic and overlapping activities of tumor necrosis factor-alpha and IL-1. J Immunol. 1988; 141:527–530. [PubMed: 3260255]

Latz E, Schoenemeyer A, Visintin A, Fitzgerald KA, Monks BG, Knetter CF, Lien E, Nilsen NJ, Espevik T, Golenbock DT. TLR9 signals after translocating from the ER to CpG DNA in the lysosome. Nat Immunol. 2004; 5:190–198. [PubMed: 14716310]

Lopera-Mesa TM, Mita-Mendoza NK, van de Hoef DL, Doumbia S, Konate D, Doumbouya M, Gu W, Traore K, Diakite SA, Remaley AT, et al. Plasma uric acid levels correlate with inflammation and disease severity in Malian children with Plasmodium falciparum malaria. PLoS One. 2012; 7:e46424. [PubMed: 23071567]

Love MS, Millholland MG, Mishra S, Kulkarni S, Freeman KB, Pan W, Kavash RW, Costanzo MJ, Jo H, Daly TM, et al. Platelet factor 4 activity against P. falciparum and its translation to nonpeptidic mimics as antimalarials. Cell Host Microbe. 2012; 12:815–823. [PubMed: 23245326]

Mariathasan S, Newton K, Monack DM, Vucic D, French DM, Lee WP, Roose-Girma M, Erickson S, Dixit VM. Differential activation of the inflammasome by caspase-1 adaptors ASC and Ipaf. Nature. 2004; 430:213–218. [PubMed: 15190255]

Martinon F, Petrilli V, Mayor A, Tardivel A, Tschopp J. Gout-associated uric acid crystals activate the NALP3 inflammasome. Nature. 2006; 440:237–241. [PubMed: 16407889]

McGilvray ID, Serghides L, Kapus A, Rotstein OD, Kain KC. Nonopsonic monocyte/macrophage phagocytosis of Plasmodium falciparum-parasitized erythrocytes: a role for CD36 in malarial clearance. Blood. 2000; 96:3231–3240. [PubMed: 11050008]

Orengo JM, Evans JE, Bettiol E, Leliwa-Sytek A, Day K, Rodriguez A. Plasmodium-induced inflammation by uric acid. PLoS Pathog. 2008; 4:e1000013. [PubMed: 18369465]

Orengo JM, Leliwa-Sytek A, Evans JE, Evans B, van de Hoef D, Nyako M, Day K, Rodriguez A. Uric acid is a mediator of the Plasmodium falciparum-induced inflammatory response. PLoS One. 2009; 4:e5194. [PubMed: 19381275]

Parroche P, Lauw FN, Goutagny N, Latz E, Monks BG, Visintin A, Halmen KA, Lamphier M, Olivier M, Bartholomeu DC, et al. Malaria hemozoin is immunologically inert but radically enhances innate responses by presenting malaria DNA to Toll-like receptor 9. Proc Natl Acad Sci U S A. 2007; 104:1919–1924. [PubMed: 17261807]

Pichyangkul S, Saengkrai P, Webster HK. Plasmodium falciparum pigment induces monocytes to release high levels of tumor necrosis factor-alpha and interleukin-1 beta. Am J Trop Med Hyg. 1994; 51:430–435. [PubMed: 7943569]

Pichyangkul S, Yongvanitchit K, Kum-arb U, Hemmi H, Akira S, Krieg AM, Heppner DG, Stewart VA, Hasegawa H, Looareesuwan S, et al. Malaria blood stage parasites activate human plasmacytoid dendritic cells and murine dendritic cells through a Toll-like receptor 9-dependent pathway. J Immunol. 2004; 172:4926–4933. [PubMed: 15067072]

Prakash D, Fesel C, Jain R, Cazenave PA, Mishra GC, Pied S. Clusters of cytokines determine malaria severity in Plasmodium falciparum-infected patients from endemic areas of Central India. J Infect Dis. 2006; 194:198–207. [PubMed: 16779726]

Rathinam VA, Jiang Z, Waggoner SN, Sharma S, Cole LE, Waggoner L, Vanaja SK, Monks BG, Ganesan S, Latz E, et al. The AIM2 inflammasome is essential for host defense against cytosolic bacteria and DNA viruses. Nat Immunol. 2010; 11:395–402. [PubMed: 20351692]

Reimer T, Shaw MH, Franchi L, Coban C, Ishii KJ, Akira S, Horii T, Rodriguez A, Nunez G. Experimental cerebral malaria progresses independently of the Nlrp3 inflammasome. Eur J Immunol. 2010; 40:764–769. [PubMed: 19950187]

Sharma S, DeOliveira RB, Kalantari P, Parroche P, Goutagny N, Jiang Z, Chan J, Bartholomeu DC, Lauw F, Hall JP, et al. Innate immune recognition of an AT-rich stem-loop DNA motif in the Plasmodium falciparum genome. Immunity. 2011; 35:194–207. [PubMed: 21820332]

Sherry BA, Alava G, Tracey KJ, Martiney J, Cerami A, Slater AF. Malaria-specific metabolite hemozoin mediates the release of several potent endogenous pyrogens (TNF, MIP-1 alpha, and MIP-1 beta) in vitro, and altered thermoregulation in vivo. J Inflamm. 1995; 45:85–96. [PubMed: 7583361]

Shio MT, Eisenbarth SC, Savaria M, Vinet AF, Bellemare MJ, Harder KW, Sutterwala FS, Bohle DS, Descoteaux A, Flavell RA, et al. Malarial hemozoin activates the NLRP3 inflammasome through Lyn and Syk kinases. PLoS Pathog. 2009; 5:e1000559. [PubMed: 19696895]

Snow RW, Guerra CA, Noor AM, Myint HY, Hay SI. The global distribution of clinical episodes of Plasmodium falciparum malaria. Nature. 2005; 434:214–217. [PubMed: 15759000]

Stashenko, P.; Dewhirst, FE.; Peros, WJ.; Kent, RL.; Ago, JM. Synergistic interactions between interleukin. J Immunol umor necrosis factor, and lymphotoxin in bone resorption. 1987. p. 1464-1468.

Tabeta K, Hoebe K, Janssen EM, Du X, Georgel P, Crozat K, Mudd S, Mann N, Sovath S, Goode J, et al. The Unc93b1 mutation 3d disrupts exogenous antigen presentation and signaling via Toll-like receptors 3,p7 and 9. Nat Immunol. 2006; 7:156–164. [PubMed: 16415873]

Taramelli D, Basilico N, De Palma AM, Saresella M, Ferrante P, Mussoni L, Olliaro P. The effect of synthetic malaria pigment (beta-haematin) on adhesion molecule expression and interleukin-6 production by human endothelial cells. Trans R Soc Trop Med Hyg. 1998; 92:57–62. [PubMed: 9692153]

van de Hoef DL, Coppens I, Holowka T, Ben Mamoun C, Branch O, Rodriguez A. Plasmodium falciparum-derived uric acid precipitates induce maturation of dendritic cells. PLoS One. 2013; 8:e55584. [PubMed: 23405174]

Vogetseder A, Ospelt C, Reindl M, Schober M, Schmutzhard E. Time course of coagulation parameters, cytokines and adhesion molecules in Plasmodium falciparum malaria. Trop Med Int Health. 2004; 9:767–773. [PubMed: 15228486]

Wu X, Gowda NM, Kumar S, Gowda DC. Protein-DNA complex is the exclusive malaria parasite component that activates dendritic cells and triggers innate immune responses. J Immunol. 2010; 184:4338–4348. [PubMed: 20231693]

HIGHLIGHTS

1. Hz causes phagolysosome destabilization, allowing gDNA and Hz access to cytosol.
2. Plasmodial gDNA and Hz activate AIM2 and NLRP3 inflammasomes respectively.
3. Parasitized erythrocytes and natural Hz induce IL-1β via NLRP3 and AIM2.

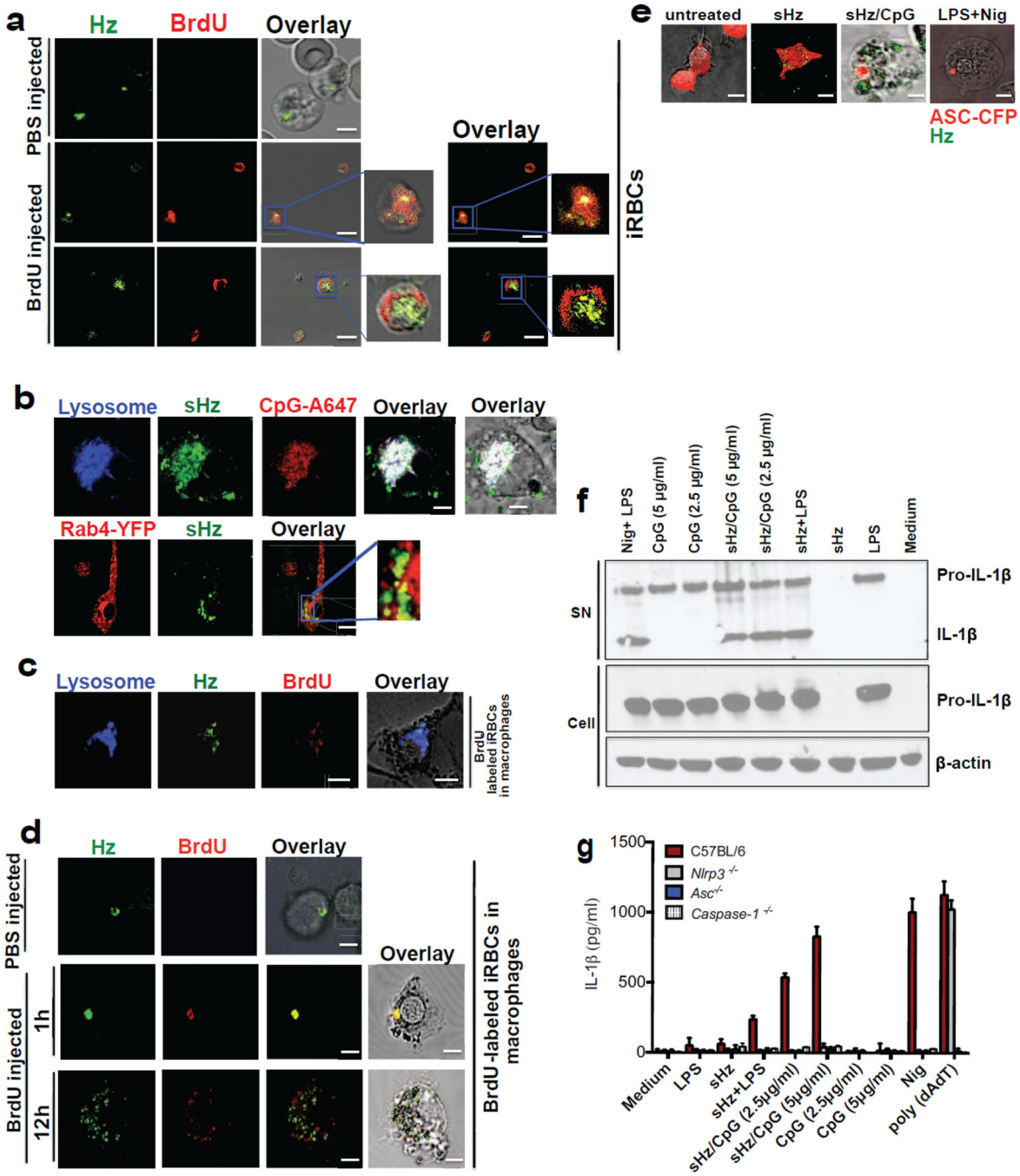

Figure 1. Hemozoin colocalizes with DNA *in vivo* is internalized into the phagolysosome where it has the capacity to prime macrophages and activate the NLRP3 inflammasome

(a)Erythrocytes from PBS injected and BrdU injected *P. berghei* ANKA infected mice were stained with FITC-conjugated anti-BrdU antibody and subjected to confocal microscopy. Boxed areas in middle and bottom panels are enlarged (3×). Scale bar: 3µm (top panel), 7.8µm (middle panel) and 7.8µm (bottom panel). (b) Top: sHz (100µg/ml) was incubated with CpG–Alexa 647 (5µg/ml) for 2h. The complex was washed 3× with PBS before incubation with immortalized BMDMs and imaged by confocal microscopy after 30 min.

Scale bar: 5μm. Bottom: Confocal microscopy of immortalized BMDMs stably transduced with Rab4-YFP, stimulated with sHz crystals (100μg/ml) for 2h. scale bar: 15μm. The boxed areas are enlarged on the right, demonstrating lack of co localization. (c) RBC from BrdU injected *P. berghei* ANKA infected mice were stained and prepared as in Fig. 1a. BMDMs were incubated with iRBCs (MOI: 5 to 1) × 1h and stained with lysotracker. Scale bar: 5μm. (d) RBC from PBS- or BrdU-injected *P. berghei* ANKA infected mice were incubated with BMDMs (MOI: 5 to 1), stained with FITC-conjugated anti-BrdU antibody and subjected to confocal microscopy after 1 or 12h. Scale bar: 20μm (top panel), 20μm (bottom panel). (e) BMDMs stably expressing ASC-CFP were treated with sHz/CpG (5μg/ml), sHz only (100μg/ml) or LPS (100ng/ml) × 2 h and then treated with nigericin (10μM), a K+ ionophore that activates NRLP3. The formation of ASC pyroptosomes was visualized by confocal microscopy. Fields are representative of at least 10 fields of view and 3 independent experiments. Scale bars from left to right: 15, 10, 5 and 5 μm; sHz (green) was visualized using reflection microscopy. (f) Immunoblot analysis of IL-1β cleavage to mature IL-1β (p17) in supernatants (SN) and cell extracts (Cell) from wt murine BMDMs stimulated as described in (g). (g) ELISA of released IL-1β by immortalized BMDMs from wt, *Nlrp3*$^{-/-}$, *Asc*$^{-/-}$ and *casp1*$^{-/-}$ macrophages which were unprimed or primed or with LPS (100ng/ml) for 2 h, and then left unstimulated or stimulated for an additional 12 h with sHz, sHz/CpG (sHz: 100μg/ml and CpG: 2.5μg/ml and 5μg/ml), CpG (2.5μg/ml and 5μg/ml) or transfected with 1.5 μg/ml poly (dAdT). Nigericin (Nig) was used as a control. Poly (dAdT) was used as an AIM2 inflammasome activating control. Data are presented as mean ± SD of triplicates and are representative of 3 independent experiments. See also Fig. S1.

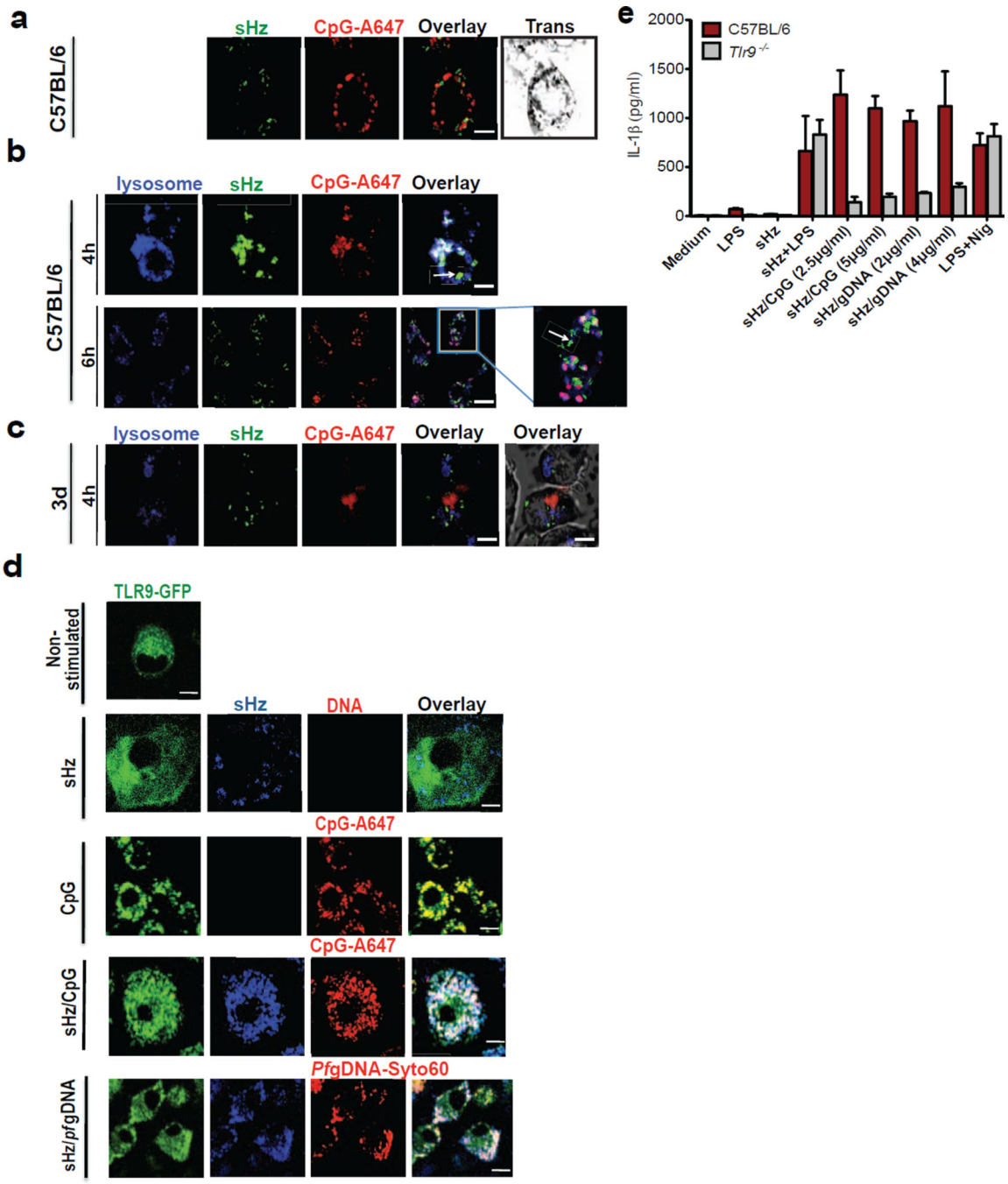

Figure 2. Synthetic Hz/CpG or sHz/*Pf* gDNA induce TLR9 translocation to the phagosome, followed by TLR9-dependent release of IL-1β

(a) sHz/CpG-A 647 (5μg/ml) was added to the cells and subjected to confocal microscopy after 6h of incubation. Scale bar: 5μm. (b) BMDMs were incubated with sHz/CpG-A 647 (5μg/ml) × 4h or 6h and stained with LysoTracker (blue). Scale bar: 10μm (top panel) and 5μm (bottom panel). Boxed area in main image at right is enlarged (2.5×); The arrow (in both top and bottom panel) indicates Hz in the cytosol. (c) "3d" macrophages, functionally deficient in TLRs 3,7 and 9, were incubated with CpG-A647 DNA × 4h. Scale bar: 10μm. Fields are representative of at least 10 fields of view and three independent experiments. (d)

Immortalized BMDMs isolated from transgenic TLR9-GFP mice were left untreated or incubated with sHz (100μg/ml), CpG-Alexa 647 (5μg/ml), sHz/CpG-Alexa 647 (5μg/ml) and sHz/*Pf* gDNA-Syto60 (4μg/ml) for 30 min and living cells were visualized by confocal microscopy. Fields are representative of at least 10 fields of view and three independent experiments. Scale bars from top to bottom: 5μm, 15μm, 5μm, 15μm and 5μm. (e) ELISA of IL-1β production by wt and *Tlr9*$^{-/-}$ BMDMs, primed or unprimed for 2 h with LPS (100ng/ml) and then left unstimulated or stimulated with indicated amounts of sHz, sHz/CpG complex, sHz/*Pf* gDNA or nigericin (10μM). Supernatants were analyzed for IL-1β 12h after stimulation. Data are presented as mean ± SD of triplicates and are representative of 3 independent experiments. See also Figure S2.

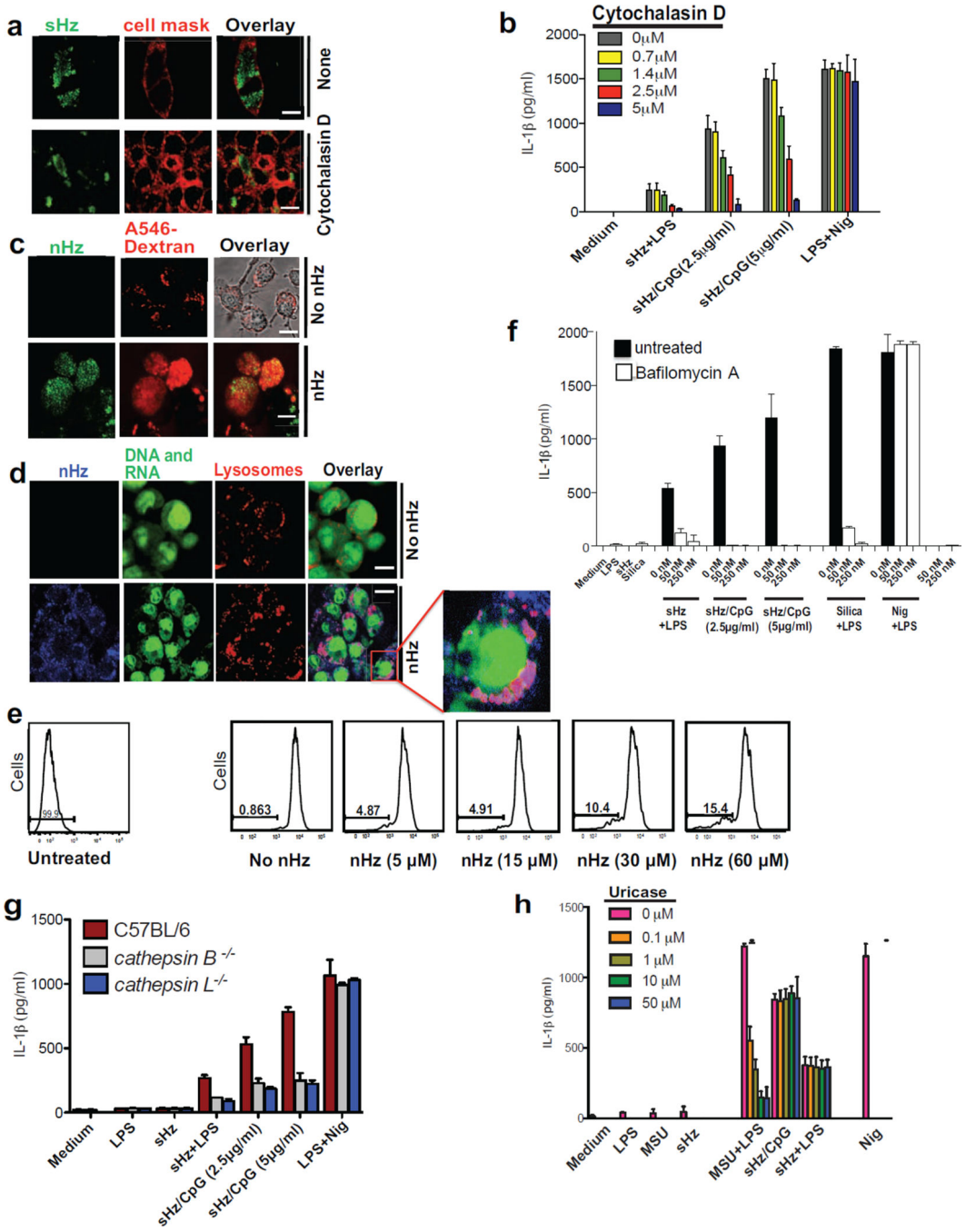

Figure 3. Phagocytosis of crystals leads to phagolysosomal destabilization and is necessary for IL-1β release

(a) Confocal microscopy of BMDMs stimulated with sHz (100μg/ml) for 2h in the absence and presence of cytochalasin D (2.5 μM). Cell membranes were stained with cell mask (red). Scale bar: 5μm (top) and 20μm (bottom). (b) ELISA of the release of IL-1β into supernatants of immortalized BMDMs left untreated or treated with increasing concentration of cytochalasin D and then stimulated for 12 h with sHz or sHz/CpG complex. (c) Confocal microscopy of immortalized BMDMs incubated with A546-Dextran 10kDa for 45 min and then either left untreated or stimulated with 100μM nHz for 4 h. Scale bar (top and bottom

panels: 10μm) (d) Macrophages were stained with acridine orange (0.05 mg/ml) for 10 min and then stimulated with nHz (100μM). 4h after stimulation, cells were analyzed by confocal microscopy. Fields are representative of at least 10 fields of view and three independent experiments. Scale bar: 10μm (top) and 20μm (bottom). Boxed area is enlarged (9×). (e) FACS analysis of immortalized BMDMs stained with acridine orange and treated with indicated amounts of nHz × 4h. The numbers above the brackets indicate the % macrophages that have lost acridine orange staining. (f) ELISA of released IL-1β from unprimed or LPS-primed immortalized BMDMs pretreated with indicated concentrations of bafilomycin A × 2 h and then stimulated with sHz, sHz/CpG or Silica (500μg/ml) × 12 h. (g) ELISA of released IL-1β by wt, *ctsb*$^{-/-}$ and *ctsl*$^{-/-}$ BMDMs left unstimulated or stimulated with sHz (100μg/ml) or sHz/CpG for 12 h. (h) ELISA of IL-1β production by unprimed or LPS-primed immortalized murine BMDMs pretreated with indicated concentrations of Uricase for 2 h, stimulated with LPS (100ng/ml) for another 2 h and then incubated with MSU (500μg/ml), sHz (100μg/ml) and sHz/CpG (5μg/ml) for 12 h. Data are presented as mean ± SD of triplicates and are representative of 3 independent experiments. See also Fig. S3.

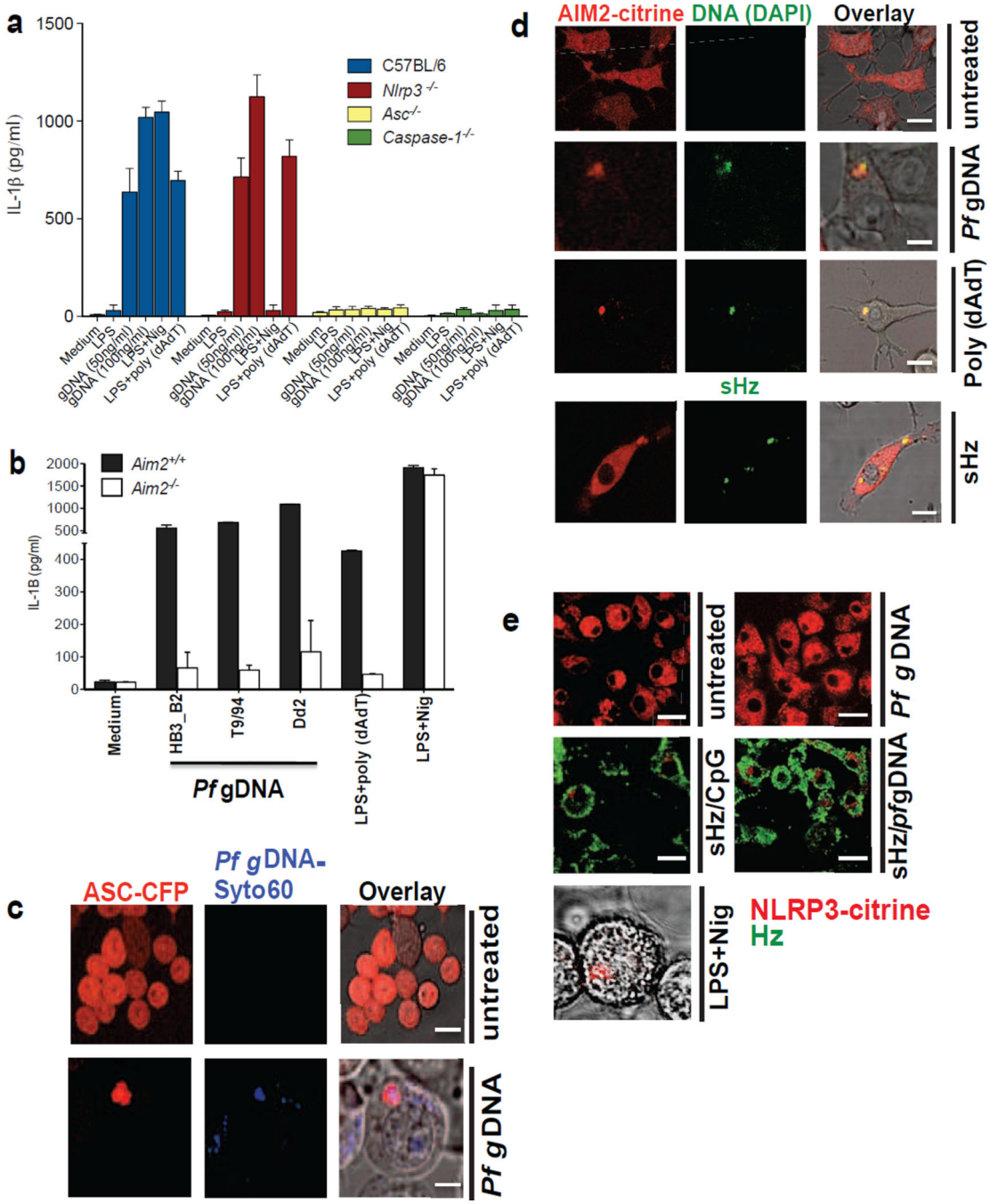

Figure 4. *Pf* gDNA induces IL-1β through activation of AIM2 inflammasome

(a) 50 and 100 ng/ml of *Pf* gDNA (3D7) were transfected using lipofectamine into LPS primed (100ng/ml × 2h) immortalized murine wt, *Nlrp3*$^{-/-}$, *Asc*$^{-/-}$ and *casp1*$^{-/-}$ BMDMs. After 12h, IL-1β was measured in the culture supernatants by ELISA. (b) 100ng/ml of gDNA from different strains of *Pf* (Dd2, T9/94, HB3-B2) was transfected using lipofectamine into LPS-primed primary *Aim2*$^{+/+}$ and *Aim2*$^{-/-}$ BMDMs. Cell culture supernatants were used to measure IL-1β using ELISA. Data are presented as mean ± SD of triplicates and are representative of 3 independent experiments. (c) Confocal microscopy of

LPS primed ASC-CFP cells left untrasfected or transfected with 100ng/ml Syto60-labeled *Pf* gDNA. Scale bar: 20μm (top), 5μm (bottom) (d) Confocal microscopy of LPS primed AIM2-citrine macrophages left untransfected or transfected with 100ng/ml DAPI-labeled *Pf* gDNA, DAPI-labeled poly (dAdT) using lipofectamine or just incubated with sHz. Scale bar (from top to bottom): 15μm, 5μm, 15μm and 15μm. (e) Confocal microscopy of NLRP3-citrine macrophages untreated or treated with sHz/CpG (5μg/ml), sHz/*Pf* gDNA (4μg/ml), nigericin or transfected with 100ng/ml *Pf* gDNA using Lipofectamine. Images are representative of at least 10 fields of view and three independent experiments. Scale bar: All 20μm except the one in the bottom which is 5μm. See also Fig. S4.

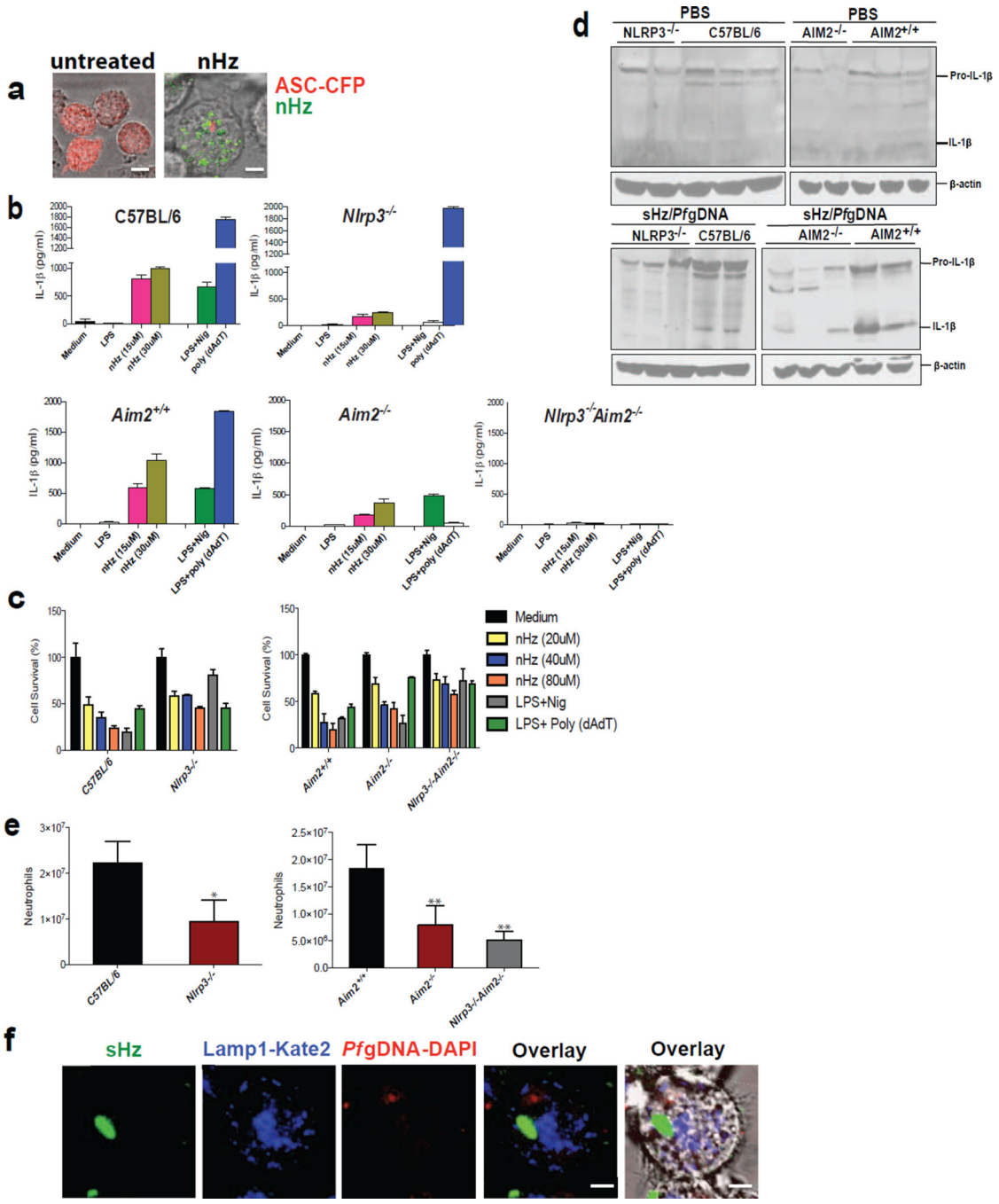

Figure 5. nHz and sHz/*Pf* gDNA complex induce IL-1β production and pyroptosis both *in vitro* and *in vivo* via NLRP3 and AIM2

(a) Macrophages stably expressing ASC-CFP were left untreated or treated with nHz (100μM). The formation of ASC pyroptosomes was visualized using confocal microscopy. Scale bar: 15μm (left) and 5μm (right) (b) Primary wt, *Nlrp3*$^{-/-}$, *Aim2*$^{+/+}$, *Aim2*$^{-/-}$ and *Nlrp3*$^{-/-}$, *Aim2*$^{-/-}$ BMDMs were incubated for 12 h with 15 μM and 30 μM of nHz, nigericin (10μM) or transfected with 1.5μg/ml poly (dAdT) using Lipofectamine. Cell culture supernatants were assessed for IL-1β release by ELISA (c) Primary wt, *Nlrp3*$^{-/-}$,

Aim2$^{+/+}$, *Aim2*$^{-/-}$, and *Nlrp3*$^{-/-}$, *Aim2*$^{-/-}$ BMDMs were incubated for 12 h with 20 μM, 40 μM and 80 μM of nHz or transfected with Poly (dAdT). Cell survival was measured using calcein AM. Medium was set as 100%. Data are mean cytokine levels ± SD of triplicate determinations and are representative of 3 independent experiments (d) wt, *Nlrp3*$^{-/-}$, *Aim2*$^{+/+}$, *Aim2*$^{-/-}$ and *Nlrp3*$^{-/-}$*Aim2*$^{-/-}$ mice were i.v. injected in the tail vein with endotoxin-free PBS or sHz/*Pf* gDNA (1mg sHz, 15μg *Pf* gDNA). After 12 h livers were dissected and homogenized. Each lane corresponds to one mouse. (e) wt (n=12), *Nlrp3*$^{-/-}$ (n=16), *Aim2*$^{+/+}$(n=9), *Aim2*$^{-/-}$ (n=14), and *Nlrp3*$^{-/-}$ *Aim2*$^{-/-}$ (n=6) mice were intraperitonally injected with sHz/*Pf* gDNA (1mg sHz, 15μg *Pf* gDNA) or PBS. After 15 h, peritoneal cells were harvested, counted and FACS analysis was performed using GR-1 antibody. Basal neutrophil influx in PBS injected mice was subtracted to determine total number of neutrophils recruited to the peritoneal cavity. Student's t-test was used to calculate P values (*p<0.05, **p<0.001). (f) *Pf* gDNA (5μg/ml) was DAPI stained for 30 min and used to make sHz/*Pf* gDNA. Lamp1-Kate2 macrophages were then stimulated with sHz/*Pf* gDNA for 2 h and subjected to reflection confocal microscopy. Fields are representative of at least 10 fields of view and three independent experiments. Scale bar: 5μm. See also Fig. S5.

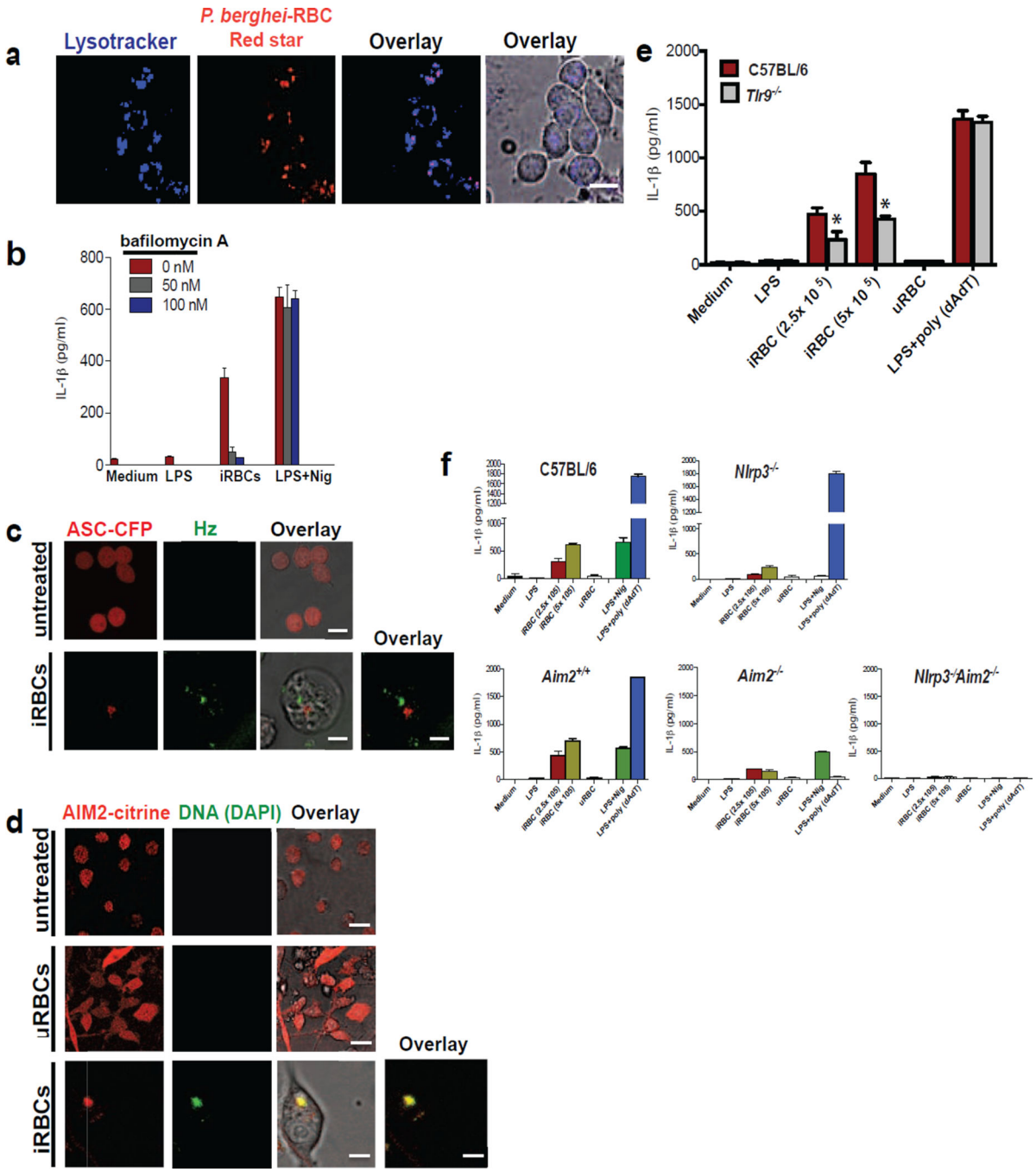

Figure 6. *P. berghei*-RBCs induced IL-1β production is NLRP3 and AIM2 dependent

(a) Confocal imaging of immortalized BMDMs incubated with 8× 10^5 *P. berghei* (NK65) Red star for 2 h. Lysosomes were stained with lysotracker (blue). Scale bar: 20μm (b) ELISA of the release of IL-1β from immortalized BMDMs pretreated with indicated concentrations of bafilomycin A for 2 h and then incubated with 8× 10^5 *P. berghei*-RBCs for 12 h (c) ASC-CFP macrophages were incubated with 8× 10^5 *P. berghei*-RBCs for 12 h and imaged by confocal microscopy. Natural Hz was visualized using reflection microscopy (green). Scale bar: 20μm (top) and 5μm (bottom) (d) *P. berghei*-RBCs (iRBCs) and

uninfected (uRBCs) were incubated with DAPI for 1h and then co-cultured with AIM2-citrine macrophages for 2 h. Fields are representative of at least 10 fields of view and three independent experiments. Scale bar: 20μm (top), 20μm (middle) and 5μm (bottom) (e) Wt and *Tlr9*$^{-/-}$ BMDMs were incubated with 2.5×10^5 and 5×10^5 *P. berghei*-infected RBCs, 5×10^5 uRBCs, or transfected with poly (dAdT) using Lipofectamine for 12 h. The supernatants were subjected to ELISA for IL-1β. *P<0.05, (Student's *t*-test) (f) Primary wt, *NLRP3*$^{-/-}$, *AIM2*$^{+/+}$, *AIM2*$^{-/-}$ and *NLRP3*$^{-/-}$, *AIM2*$^{-/-}$ BMDMs were incubated with 2.5×10^5 and 5×10^5 *P. berghei*-RBCs, 5×10^5 uRBCs for 12 h or transfected with poly (dAdT) using Lipofectamine. The supernatants were subjected to ELISA for IL-1β. Infected RBCs used for all experiments above were taken at day 14 from C57BL/6 mice infected with *P. berghei* NK65. Data are presented as the mean of triplicate determinations ± SD and are representative of 3 independent experiments. See also Fig. S6.